Critical behaviour of metallic liquids

1990 J. Phys.: Condens. Matter 2 SA33

(http://iopscience.iop.org/0953-8984/2/S/004)

J. Phys.: Condens. Matter **2** (1990) SA33–SA45. Printed in the UK

Critical behaviour of metallic liquids

F Hensel
Institute of Physical Chemistry and Centre of Material Science, Philipps-University, D-3550 Marburg, Federal Republic of Germany

Received 9 July 1990

Abstract. Experimental results for fluid metals near the liquid–vapour critical point show that profound changes in the electronic structure of fluid metals occur in that region. A gradual transition from metallic to non-metallic behaviour occurs with decreasing density, which manifests itself in a correspondingly strong thermodynamic state dependence of the effective interparticle interaction. It will be shown that this strong dependence noticeably influences the thermodynamic and kinetic features of the vapour–liquid phase transition of fluid metals. Special emphasis will be given to the interplay between the critical point density fluctuations and the change in the electronic properties in the course of the metal–non-metal transition.

1. Introduction

Whilst considerable progress has been made over the last decades in understanding the behaviour of molecular fluids near critical points [1, 2], the nature of the phase transition of metallic fluids at the liquid–vapour critical point is relatively less well understood. A fundamental distinction between metallic fluids and their molecular insulating counterparts lies in the character of interparticle interactions. Far below the liquid–vapour critical point, when the density difference between coexisting phases is large, two transitions occur at once when the metallic liquid condenses from the insulating vapour. One of these is the liquid–vapour transition and the other is the metal–insulator transition. The occurrence of the latter implies that the interparticle interactions are very different in the two phases. The metal atoms in the dilute insulating vapour are merely highly polarizable atoms interacting through weak van der Waals interactions, whereas valence electrons in the metallic liquid are dissociated and the cohesive forces are thought to arise from screened Coulomb potentials. By contrast, for molecular fluids, such as Ar, the interaction potential energy function may be considered to be independent of density to a good approximation. This contrast was first discussed by Landau and Zeldovitch [3] who suggested the possibility of separate first-order electronic and liquid–vapour transitions in fluid metals. Subsequent theoretical attempts to model the statistical mechanics of the metal–insulator transition in fluids reach similar conclusions but are still insufficient to provide a clear-cut answer to this question from theory (for reviews with many references see, e.g., [4]).

In the absence of an adequate theory, the obvious alternative is to explore the matter experimentally. Several attempts have been made during the past two decades to determine the basic phase behaviour of fluid metals, namely the equation of state,

0953-8984/90/SA0033 + 13 $03.50

Table 1. Critical temperatures, pressures and densities of some metals.

Metal	T_c (K)	p_c (MPa)	ρ_c (g cm^{-3})	Reference
Hg	1751	167.3	5.8	[5]
Cs	1924	9.25	0.38	[6]
Rb	2017	12.45	0.29	[6]
K	2280	16.1	0.19	[7]
Na	2485	24.8	0.30	[8]

together with the basic electronic properties such as the electrical conductivity, but the subject has remained elusive until quite recently. The difficulties are immediately evident from a glance at table 1. A combination of high temperatures and pressures is required to bring a fluid metal sample somewhere near its critical point. The critical temperatures and pressures are low enough to be studied under static conditions for only a very few metals (Hg, Cs, Rb, K and Na) but, even for these systems, the accuracy with which properties can be measured is severely limited by the highly reactive nature of metals at high temperatures and by the severe problems with the control and measurement of temperature in any high-temperature high-pressure experiment. The latter becomes particularly important in studies close to the critical point where the analysis of experimental measurements can easily be hampered by the presence of spurious effects due to temperature gradients. It is therefore not surprising that relatively accurate experimental results in the critical region are available for only the three metals with the lowest critical points: monovalent Cs and Rb and divalent Hg. The experimental information for these metals is accurate enough to permit determination of the asymptotic behaviour of the properties near the critical point.

The general subject of the metal–insulator transition in low-density metals has repeatedly been reviewed in the literature [9–15]. Therefore, an extended review of the subject is unnecessary. Instead I have selected for attention those novel developments which have not been adequately reviewed elsewhere, e.g. liquid–vapour asymmetries in fluid metals and studies of the interplay between the liquid–vapour critical point density fluctuations and the change in the electronic properties in the course of the metal–insulator transition.

2. Divalent metals

As table 1 shows, mercury has the lowest critical temperature of any fluid metal. For this reason it has proven to be an important substance for investigation of the metal–insulator transition of a divalent metal at low densities and for study of the relationship between the microscopic electronic structure and the liquid–vapour phase transition.

The physical consequences of the strongly state-dependent electronic structure in the course of the metal–insulator transition are vividly illustrated by data such as those displayed in figure 1. These plots show a selection of the most accurate density ρ (figure 1(*a*)) and DC electrical conductivity (figure 1(*b*)) data in the form of isotherms as a function of pressure at subcritical and supercritical temperatures. Near the critical point the conductivity drops sharply, showing a strong effect of the phase transition on

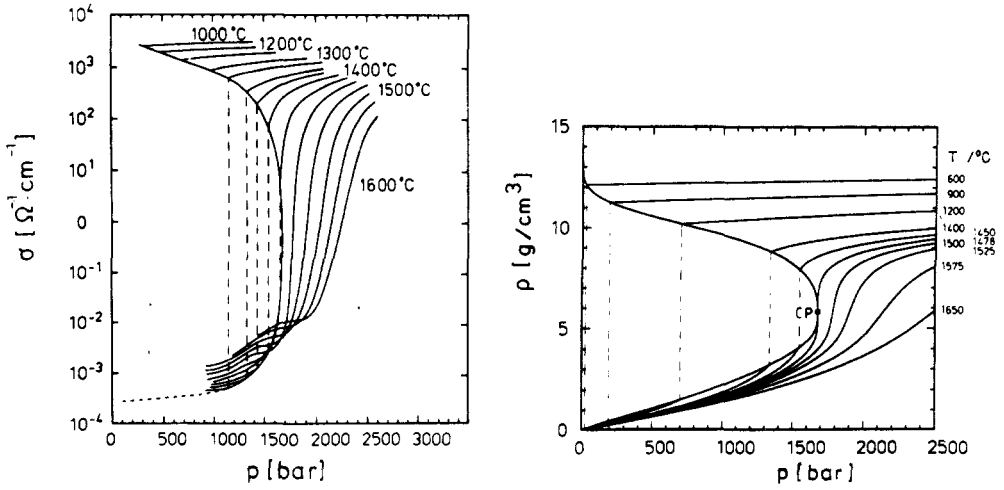

Figure 1. (*a*) Equation-of-state data of fluid mercury at subcritical and supercritical temperatures as a function of pressure. (*b*) Electrical conductivity isotherms of fluid mercury at subcritical and supercritical conditions.

the electronic structure. Nevertheless, there is no indication of a discontinuity in the electronic character within the present limits of experimental resolution. Except across the liquid–vapour phase boundary, the metal–insulator transition is continuous. The data shown in figure 1 illustrate the qualitative relationship between rapid variations in the conductivity σ and density ρ and suggest that density is the dominant factor governing the metal–insulator transition.

The separate effects of temperature and density are shown in figure 2 representing isothermal plots of σ versus ρ. At the highest density $\rho = 13.6$ g cm^{-3}, corresponding to the liquid range near room temperature, the conductivity is about $10^4\ \Omega^{-1}$ cm^{-1} and free-electron theory gives an electron mean free path λ of about 7 Å which exceeds only slightly the mean interatomic spacing. Application of the nearly-free-electron (NFE) model leads to the conclusion that σ can be satisfactorily explained within the context of the Ziman theory if the effect of the atomic d states is included in the pseudopotential [16]. Mercury is thus essentially a NFE metal, despite the comparatively small mean free path. The NFE character is further confirmed by the observation that in this density range the low-frequency optical conductivity $\sigma(\omega)$ shows Drude-like behaviour [17] and the Hall coefficient R_H [18] retains the free-electron value. A comparision of the density dependence of σ, $\sigma(\omega)$, R_H and the Knight shift K [19] shows that for densities down to about 11 g cm^{-3} the properties of mercury can be described by the NFE theory of metals but, with further decreasing density, a rather gradual diminution of metallic properties occurs in the density range between 11 and 9 g cm^{-3}. For still smaller densities, the behaviour of σ, $\sigma(\omega)$ and K is characteristic of a substance with semiconducting properties.

As is well known, this type of metal–semiconductor transition is predicted by the Bloch–Wilson band model to occur for an expanded divalent metal such as mercury when the 6s valence and 6p conduction bands no longer overlap. In a crystal, a real energy gap appears and widens as the density decreases. Mott [20] has proposed that the general features of the crystalline model survive in the liquid state with band edges

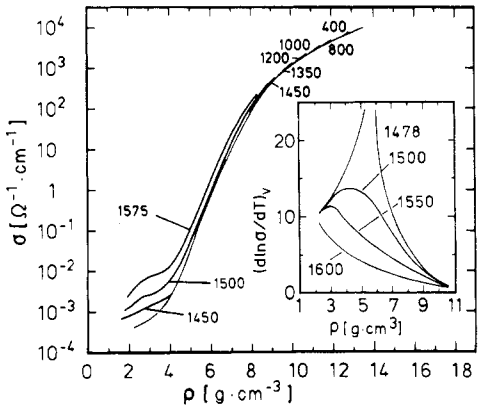

Figure 2. Electrical conductivity σ of fluid mercury at constant subcritical and supercritical temperatures as a function of density ρ. The temperatures are in degrees Celsius. The inset shows the constant-volume temperature coefficient $[\partial(\ln\sigma)/\partial T]_V$ at constant temperatures as a function of density.

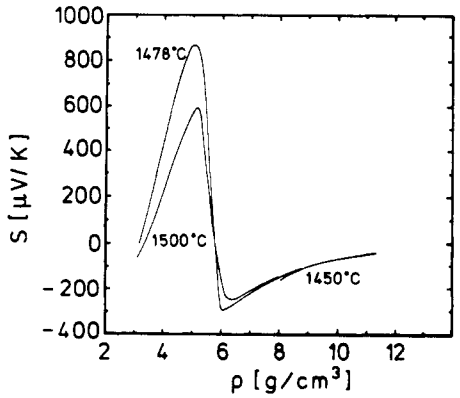

Figure 3. Thermopower S of fluid mercury at constant temperatures close to the critical point as a function of density.

smeared out by disorder. Thus, the density $N(E)$ of states is expected to tail into the gap owing to the loss of long-range order. The tails overlap in the region of Fermi energy E_F replacing the real energy gap of the crystal by a pseudogap or a minimum in $N(E)$ at E_F. The pseudogap depends strongly on density. When the magnitude of $N(E)$ in the pseudogap decreases with sufficient expansion to a negligibly small value, the optical properties of mercury must become compatible with the opening up of an energy gap. The latter is observed for expanded mercury for densities lower than 9 g cm^{-3}. For these densities the shape of the $\sigma(\omega)$ curves is characteristic of a substance either with a real energy gap or with a range of energies, which is so thinly populated with states that their contribution to the optical properties is negligibly small. This view is completely consistent with the observation of a sharp drop in the Knight shift [19] for densities smaller than 9 g cm^{-3}.

In principle, one might hope to determine the energy gap experimentally by identifying it with the activation energy of the conductivity which successfully describes the temperature dependence of the conductivity in crystalline and amorphous solid semiconductors. However, in high-temperature liquids such as mercury not too far from its critical point, strong fluctuations in local density become important. Hence, the application of solid state concepts suffers from serious limitations. This is evident immediately on consideration of the constant-volume temperature coefficient $[\partial(\ln\sigma)/\partial T]_V$ plotted versus the density in the inset in figure 2 for various temperatures. The strong temperature dependence of $[\partial(\ln\sigma)/\partial T]_V$ around the critical density of 5.8 g cm^{-3} is an obvious indication of the strong interplay between the liquid–vapour critical density fluctuations and the electrical characteristics.

Be that as it may, it is obvious from figure 2 that σ falls more rapidly as the density decreases below 9 g cm^{-3}. The increase in the gap with decreasing density leads to a rapid decrease in the number of thermally excited charge carriers, implying that the scattering must change dramatically from scattering by screened ions to scattering

by neutral atoms. As a result, the electrical transport is affected by two drastic and inextricably connected changes in the number density n and mobility μ of charge carriers. For a given species of charge carriers, the latter two quantities determine the conductivity according to $\sigma = ne\mu$ but, besides the trivial effects of the changes in the number density of thermally excited electrons and of the related change in the scattering process from that of ionic scattering centres to neutral scattering centres, an additional effect which is connected with the liquid–vapour critical point density fluctuations begins to play a role. Cluster of mercury atoms are assumed to localize the thermally excited electrons, i.e. the electron can be trapped by density fluctuations. These clusters involving self-trapped electrons are quite analogous to the polarons in solid state physics, except that the likelihood of forming such states is greatly enhanced by the high mobility of atoms in the fluid state. Self-trapping occurs because the interaction of the electron with the fluid atoms distorts the fluid structure and creates regions which localize the electron. The entropy changes induced by this effect can strongly influence the thermal transport of the electrons.

The entropy effect becomes in particular visible in the behaviour of the thermopower of mercury in the density range where fluid mercury behaves as a slightly ionized fluid (figure 3). In this region, with both trapped and delocalized electrons present, the delocalized electrons contribute a thermopower

$$S_f = -(k/e)[(E_c - \eta)/kT + c] \tag{1}$$

where E_c is the bottom of the continuum states, η is the chemical potential, and c is a constant of order one while the self-trapped electrons contribute

$$S_T = -(k/e)[(E_c + \Delta F - \eta)/kT + \Delta\sigma/k] \tag{2}$$

where ΔF and $\Delta\sigma$ are the free energy and entropy changes due to self-trapping of the electron. It is obvious that, because $\Delta\sigma/k$ is a substantial negative quantity, the self-trapped electrons give a large positive contribution to the thermopower. The polaron-type effect, with an electron changing the local density of a few atoms around it, leads to a negative heat of transport which is present only if the density of charge carriers is small enough that they do not compete unduly for the surrounding neutral atoms. The negative heat of transport arises because the fast electrons interact with the fluid mercury surroundings less strongly than the slow electrons and carry less heat with them.

The dominance of density fluctuations in determining the physical properties of metals in the critical region becomes especially evident in the behaviour of the optical properties of mercury [21–24]. At very low densities a line spectrum is observed with the main absorption lines at 4.89 and 6.7 eV corresponding to transitions between the 6s ground state and the 6p triplet and singlet state of the Hg atom. As the density is increased, the sharp lines broaden owing to interactions with neighbouring atoms, resulting in a relatively steep absorption edge, which moves rapidly to lower energies with increasing density. Detailed analysis of the data [25, 26] shows, in fact, that a uniform density increase is insufficient to explain the observed line broadening. Clusters of atoms created by density fluctuations have to be explicitly taken into account. The absorption edge is then lowered by the environment of the atom being excited, and the edge is thus explained in terms of absorption by excitonic states of large randomly distributed clusters. From the large values of the absorption coefficient it can be concluded that the singlet exciton (6^1p_1) with large oscillator strength broadens faster than the triplet exciton (6^3p_1) with small oscillator strength.

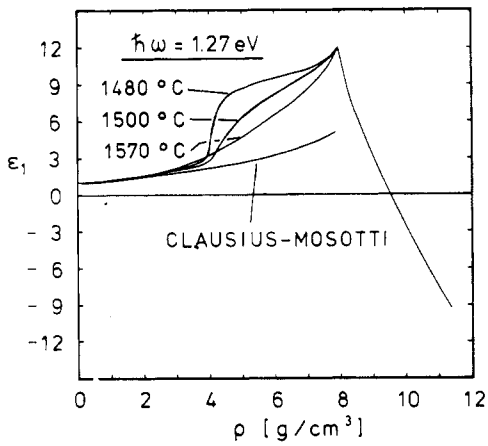

Figure 4. Real part of the dielectric constant ε_1 of fluid Hg at constant photon energy $\hbar\omega = 1.27$ eV as a function of density at constant temperatures.

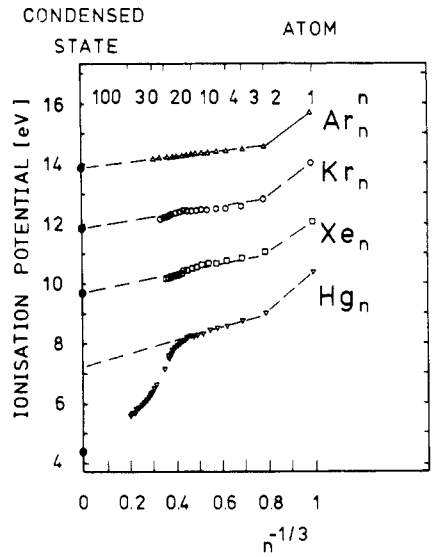

Figure 5. Comparison of the size dependence of the effective ionization potentials of clusters of Ar, Kr, Xe [28] and Hg [29, 30]. The ionization potential is plotted versus the reciprocal cube root of the number of atoms in the cluster.

The shift of the effective optical gap and temperature- and density-induced changes in the shape of the optical absorption spectrum can be viewed equivalently in terms of a linear enhancement of ε_1. Specifically, ε_1 may be obtained from the standard Kramers–Kronig integral over the frequency-dependent optical conductivity. Experimental data for ε_1 of mercury at a constant photon energy of 1.27 eV are shown in figure 4 in the form of isotherms plotted versus density. There is an obvious indication in these data of the interplay between the critical density fluctuations and the behaviour of ε_1. At the lowest least-metallic densities, ε_1 is only slightly depending on temperature and follows the Clausius–Mosotti model of the dielectric constant of induced dipoles. Then there is a strongly temperature-dependent upward deviation from Clausius–Morsotti behaviour. The fall to the negative values seen in the metallic state at around 9 g cm^{-3} is quite gradual. The most characteristic feature of the data is the strong temperature dependence of ε_1 close to the liquid–vapour region. Figure 4 shows clearly the presence of a large anomalous critical contribution to ε_1 which close to the critical isochore at a temperature about 0.1% above T_c reaches a maximum of about 70% of the background. A non-metallic substance such as CO, in contrast, exhibits only a very weak critical dielectric anomaly of 0.1% at a corresponding distance from the critical point [27]. This contrast reveals the strong interplay between the vapour–liquid critical point fluctuations and the large change in electronic structure associated with the gradual metal–insulator transition.

This dominance of density fluctuations in determining the physical properties in the critical region of mercury leads us to consider the properties of small clusters of metal atoms. Because of its closed-shell (divalent) atom configuration, it can be expected that small clusters of mercury are insulating and bonded through weak van der Waals

forces. This feature contrasts clearly with the metallic properties associated with the corresponding bulk material. Thus a size-dependent insulator–metal transition can be expected to occur in these clusters. The relation of cluster size of the valence electronic structure of non-interacting isolated clusters has been studied directly by employing modern supersonic beam techniques. For example the ionization thresholds for argon, krypton, xenon [28] and mercury clusters [29, 30] produced in supersonic beams are shown in figure 5. Here the ionization energies determined by energy-resolved mass spectrometry [29] and by photoelectron–photo-ion coincidence spectroscopy are plotted as a function of the cube root of the reciprocal number density. It is immediately evident from a glance at figure 5 that, for small clusters of mercury atoms, one can distinguish between two extreme situations, i.e. the metallic and the van der Waals-type modifications. Mercury atoms have an s^2 atomic configuration that is widely separated in energy from the first unoccupied atomic p orbital, and so they give rise to small clusters with fully occupied van der Waals-type weakly binding s bands. The change to the observed bulk metal properties of large Hg_n clusters ($n > 110$) can only be achieved via overlap of the full s-derived valence band and the empty p-derived conduction band. The experimental results indicate that for Hg_n clusters the electronic properties of the bulk metal evolve gradually with increasing particle size in the size range $13 < n < 110$. The strong variation in the electronic structure in course of this transformation from non-metallic to metallic properties is also evidenced by studies of inner shell 5d autoionization spectra [31], of optical absorption spectra [32] and of the atomic cohesion energy [33] of mercury clusters as functions of size.

The strong variation in the electronic structure with cluster size influences also the kinetic features of the vapour–liquid phase transition of mercury. Measurements of the critical supersaturation for the homogeneous nucleation of mercury in the temperature range 260–400 K [34] show that none of the current theories for homogeneous nucleation satisfactorily predicts the observed critical supersaturations. The measured values are about three orders of magnitude lower than the values predicted by the conventional Becker–Döring–Zeldovitch (BDZ) theory. It is noteworthy that the change in the value of the bulk liquid surface tension necessary to bring the classical nucleation theory in agreement with the experimental observation is about 40%. In contrast, most molecular liquids require only a very small adjustment of the bulk liquid surface tension to bring nucleation theory and experiment into agreement. An important difference between mercury and the molecular fluids is that in the former the size-dependent metal–non-metal transition occurs in small clusters. Profound changes in the electronic structure of small clusters take place with increasing size, which manifest themselves in a correspondingly strong size dependence of all properties, most probably also including density and surface tension. Any rigorous theory of nucleation of metal vapours must take into account that the very existence of the size-dependent metal–non-metal transition noticeably influences the homogeneous nucleation process in supersaturated metal vapours. The kinetic formalism of the BDZ theory can possibly be retained, but the formation Gibbs free energies of small clusters containing 2–100 atoms must be calculated *ab initio* employing direct statistical mechanical evaluation of the partition functions of these small clusters, a procedure which is even difficult to realize for molecular clusters as large as those important in nucleation processes. However, for metal clusters the situation is even more complicated because in contrast to most molecular clusters, for which to a first approximation the behaviour can be described by reference to a single simple dispersion interaction potential for all cluster sizes, in metal clusters the effective interaction becomes size dependent. The occurrence of the non-metal–metal transition with increasing size implies that the nature of the interparticle

interaction must change dramatically from a van der Waals-type to metallic interaction. The nucleation process in supersaturated metal vapours is fundamentally distinct from that of molecular vapours in that the interparticle potentials in the critical condensation nucleus are not quantities related to intrinsically atomic properties but rather depend strongly on the nature of the electronic structure of the cluster.

3. Monovalent metals

A considerable amount of effort has been centred on the experimental and theoretical investigation of fluid alkali metals, despite the severe experimental difficulties associated with their highly reactive nature. One reason for their importance is the monovalency of alkali metals. With a single electron per atom they closely resemble the expanded crystals with half-full bands considered by Mott [35] in his original discussion of the metal–non-metal transition due to correlation. Most of the effort has focused on caesium because of its relatively low critical temperature. Measurements such as those of the electrical conductivity [36], the equation of state [37], the magnetic susceptibility [38], the Knight shift [39], the optical reflectivity [40] and the structure factor [41] have been studied as functions of temperature and pressure up to and beyond the critical point. The combined analysis of these data reveals that precursors of the metal–non-metal transition, i.e. many-electron correlations of the type invoked in the theory of the Mott–Hubbard transition [35], play an essential role in determining the electronic properties of the expanded metallic liquid for densities $\rho \leqslant 1.3\ \mathrm{g\ cm^{-3}}$, i.e. far before the metal–non-metal transition occurs close to the critical point ($\rho_c = 0.38\ \mathrm{g\ cm^{-3}}$). As in the case of divalent mercury, a distinction between different conduction mechanisms in the critical region of caesium is complicated, however, because of the strong interplay between the vapour–liquid critical point density fluctuations and the rapid change in the electronic structure as the metal–non-metal transition is approached in the critical region. Magnetic susceptibility and optical absorption measurements for alkali metals in the vapour phase show, for example, that a high concentration of molecular associates forms as the vapour density increases. These clusters have ionization energies substantially lower and electron affinities substantially higher than the corresponding values of the single atom [42]. This effectively increases the probability of electron transfer from an atom to a large cluster. The formation of a large portion of neutral or charged diamagnetic aggregates in the critical region of fluid alkali metals is completely consistent with the behaviour of the magnetic properties [38]. Thus, the conductivity observed at the critical density of Cs may be due to electrons from ionized Cs clusters [43]. A more extended review of work on alkali metals is unnecessary because reference may be made for further details to surveys that exist [4, 9, 10].

4. Liquid–vapour asymmetries in fluid metals

The occurrence of the metal–non-metal transition in expanded fluid metals implies that the electronic structure of the coexisting phases, liquid and vapour, may be fundamentally different. Under ordinary conditions, far below the critical point temperature, the liquid is metallic and the interparticle interaction is dominated by screened Coulomb potentials. In contrast, the coexisting vapour phase is insulating and can be described quite well by weak van der Waals interactions. Both of these interactions are

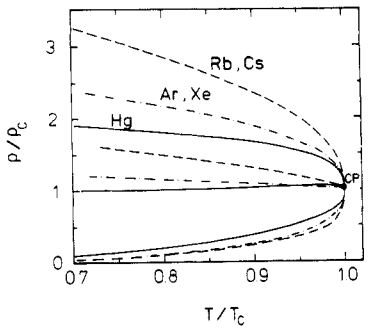

Figure 6. The reduced densities of the coexisting vapour and liquid of the inert gases Ar and Xe compared with those of the metals Cs, Rb and Hg. The plot also shows the mean value of the liquid vapour densities $\rho_d = \frac{1}{2}(\rho_L + \rho_V)$.

sufficiently short ranged, as they are in nearly all molecular fluids. As a consequence, critical phenomena typical of molecular fluids, which belong to the same universality class as certain magnetic systems, namely the universality class of the three-dimensional Ising model, can be expected. However, both types of interaction change in the course of the metal–non-metal transition, and it is this thermodynamic state dependence of the effective interparticle interaction which may have a strong influence on the liquid–vapour critical point phase transition.

The most significant experiments relevant to the effect of the liquid–vapour interparticle asymmetry and to the question of the validity of an approximate law of corresponding states are those on the liquid–vapour coexistence curves of the alkali metals caesium and rubidium [44] and of divalent mercury [45]. As mentioned above, the two fluid alkali metals exhibit metallic properties at densities near that of the critical point, in contrast to mercury, in which the gradual metal–semiconductor transition occurs in the liquid phase and which is more like a slightly ionized dense fluid in the critical region.

Despite extreme conditions at the critical points of fluid metals, the liquid–vapour coexistence curves have been measured to a resolution $\tau = |T - T_c|/T_c \simeq 5 \times 10^{-4}$, which is close enough to demonstrate the important differences between metallic and insulating molecular fluids. Figure 6 shows a reduced plot (ρ/ρ_c versus T/T_c) of the coexisting liquid densities ρ_L and vapour densities ρ_V together with the curve of the mean densities $\rho_d = \frac{1}{2}(\rho_L + \rho_V)$ versus the reduced temperature for the metals caesium, rubidium and mercury and for the inert gases argon and xenon. The curves for the metals have been established indirectly from the intercepts of measured isochores with the vapour pressure curve. The density values have been assigned to the respective liquid and vapour branches of the coexistence curve by comparing the slopes of the isochores with those of the vapour pressure curve at the point of intersection.

The diagram in figure 6 demonstrates that the reduced plots for rubidium and caesium coincide accurately, showing that a principle of corresponding states is valid for these two monovalent metals of the same group, but poor reduced correlation between the alkali metals and the inert elements argon and xenon is observed. The coexistence curves for the alkali metals are extremely asymmetric and exhibit significantly larger order parameter amplitudes. The coexistence curve for mercury differs from those of both the non-metallic fluids and the alkali metals. Thus the experimental evidence shows that metals and non-metals cannot be included together in a group obeying a principle of corresponding states, and furthermore that reduced correlations are unlikely to hold for liquid metals as a group.

The reduced diagram in figure 6 demonstrates a second interesting consequence of the strong thermodynamic state dependence of the effective particle interaction in

metallic fluids as the critical region is traversed. Fluid metals violate the hundred-year-old empirical law of rectilinear diameter [46] over a surprisingly large temperature range. By contrast, the deviations from this law are extremely (mostly immeasurably) small for the coexistence curves of essentially all non-metallic one-component fluids [47].

The law states that the locus of the tie-line midpoints $\rho_d = \frac{1}{2}(\rho_L + \rho_V)$ is a linear function of T. Since both ρ_L and ρ_V approach the limiting density ρ_c at the liquid–vapour critical point, the law can be written

$$\rho_d - \rho_c = D_1 \tau \tag{3}$$

where $\tau = T_c - T/T_c$ and D_1 is a constant. Modern theory of liquid–vapour critical phenomena based on certain solvable lattice models [48], thermodynamic arguments [49] and renormalization group studies [50] permits calculation of the diameter anomaly including effects of large-scale density fluctuations. The theory predicts that the temperature derivative of the diameter $d\rho_d/dT$, diverges at least as fast as the constant-volume specific heat c_V. That is, as the reduced temperature τ goes to zero, the diameter varies as

$$\rho_d - \rho_c = D_0 \tau^{1-\alpha} + D_1 \tau + \ldots \tag{4}$$

where $\alpha = 0.11$ is the same exponent that describes the behaviour of the constant-volume specific heat c_V. Since $1 - \alpha = 0.89$ is not very different from unity, the true singularity is difficult to separate from the analytic temperature term. The coefficient D_1 does not even have to be much larger than D_0 for the analytic term to dominate the entire range accessible to experimentation. The latter causes the difficulty in observing the $1 - \alpha$ singularity for most non-metallic fluids (see, e.g., the inert gases Ar and Xe in figure 6), and it was only with high-precision experiments on Ne, N_2, C_2H_4 and C_2H_6 [47] that it was possible to reveal that singularities with the predicted exponent $1 - \alpha$ do indeed exist for non-conducting [2] molecular fluids, i.e. that $D_0 \neq 0$ for these fluids as well. Analysis of these data [2] has led to the suggestion that many-body interactions lead to the anomalous $\tau^{1-\alpha}$-term in these fluids. In particular, it is believed that the symmetry breaking present in these fluids owing to many-body dispersion forces may be understood in terms of a thermodynamic-state-dependent effective pair interaction. Consequently, there seems to be a natural connection between this explanation and the observation of very large amplitudes of the diameter anomalies in fluid metals where the occurrence of the metal–non-metal transition implies a strong variation in the interparticle interaction.

It is evident from a glance at figure 7 that the diameter anomalies in the alkali metals, caesium and rubidium, are characterized by exponents $1 - \alpha$. The anomalies are so strong that a nearly pure power-law behaviour is seen over several decades in the reduced temperature τ. It is certainly tempting to speculate [51] that the strong dependence on density of the effective interparticle potentials in the range of the gradual metal–insulator transition is responsible for the large amplitude D_0 of the $\tau^{1-\alpha}$-term in caesium and rubidium.

The liquid–vapour coexistence curve of mercury is known with an accuracy comparable with that of the alkali metals. It is evident from figures 6 and 7 that the coexistence curve of mercury is much more symmetric than that of caesium and rubidium. Far below the critical temperature, the diameter has a positive slope as is observed for molecular fluids and for the alkali metals. In this region of temperature, when the density difference between the coexisting phases is large, the coexisting liquid is metallic ($\rho_L \geq 11$ g cm^{-3}), while the insulating vapour consists of atoms interacting through weak van der Waals

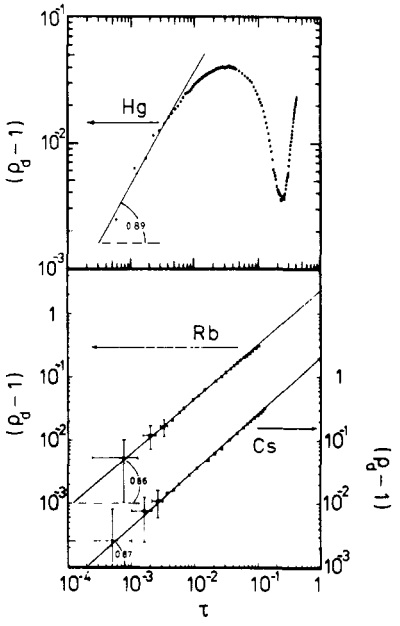

Figure 7. Power-law analysis of the diameter of caesium, rubidium and mercury.

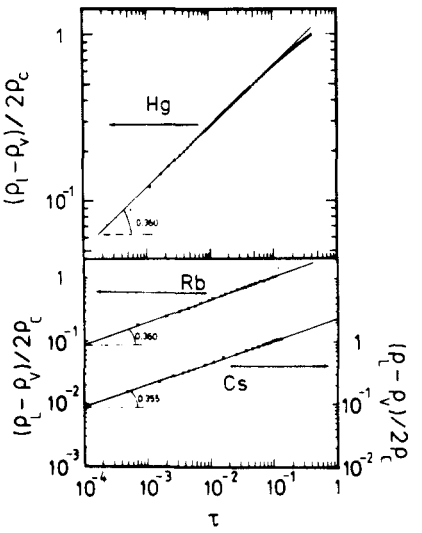

Figure 8. Power-law analysis of the order parameters of caesium, rubidium and mercury.

forces. At higher temperatures, where the liquid is in the electronic transition range, the diameter actually slopes towards higher densities, opposite to the behaviour of molecular fluids and fluid caesium and rubidium.

It is seen from figure 7 that close to the critical point of mercury the behaviour of the diameter is described by the $D_0\tau^{1-\alpha}$-term with a positive D_0. The competing variations in the electronic structure of mercury with density and temperature cause a strong wiggle at intermediate values of the reduced temperature τ. It seems reasonable to assume that the skewing of the diameter towards higher densities in the metal–non-metal density transition region between 11 and 8 g cm^{-3} is connected with the strong volume dependence of the energy gap between the 6s and 6p bands which leads to a contribution to the configurational or thermal pressure of the system. The broadening of the 6s band with decreasing volume is a result of the repulsive forces between mercury atoms at small interatomic separations. Consequently, excitation of electrons into the 6p state, whose energy is decreasing with increasing volume, has the effect of removing some of this repulsion, thereby lowering the pressure. The decrease in repulsion may be viewed as a decrease in the effective hard-core diameter of the atoms or as a softening in the effective interparticle forces.

The presence of the strong liquid–vapour interparticle asymmetry in metals does not, however, imply that the shapes of their coexistence curves cannot be described with the same exponents β as a molecular fluids:

$$\rho_L - \rho_V = B\tau^{\beta} \tag{5}$$

which describes the divergence of the order parameter approaching the critical point. Any speculation that the critical points of metals could fall into a different universality

class from the insulating molecular fluids is clearly not true as is demonstrated by figure 8. The parameter β lies between 0.35 and 0.36, a value only slightly higher than that found for the three-dimensional Ising model. Since these values are determined by single power-law fits for the range of temperatures accessible experimentally for metals, it would be modified by allowance for corrections because the data do not extend to the true critical region. The presence of strong state-dependent interactions in metals becomes visible mainly in the behaviour of the diameter. The main difference between the coexistence curves of molecular and metallic fluids is the magnitude of the coefficient D_0 in equation (4).

Acknowledgments

Financial support by the Deutsche Forschungsgemeinschaft and the Fonds der Chemischen Industrie is gratefully acknowledged.

References

[1] Levelt Sengers J M H, Morrison G and Chang R 1983 *Fluid Phase Equilibria* **14** 19
[2] Goldstein R E and Parola A 1988 *J. Chem. Phys.* **88** 7059
[3] Landau L and Zeldovitch G 1943 *Acta Phys. Chem. USSR* **18** 1940
[4] Yonezawa F and Ogawa T 1982 *Prog. Theo. Phys., Suppl.* **72** 1
Hensel F and Uchtmann H 1989 *Ann. Rev. Phys. Chem.* **40** 61
Pratt R M 1990 *Ann. Rev. Phys. Chem.* **41** at press
[5] Götzlaff W, Schönherr G and Hensel F 1988 *Z. Phys. Chem., NF* **156** 219
[6] Jüngst S, Knuth B and Hensel F 1985 *Phys. Rev. Lett.* **55** 2160
[7] Freyland W and Hensel F 1972 *Ber. Bunsenges. Phys. Chem.* **76** 347
[8] Binder H 1984 *Doctoral Thesis* University of Karlsruhe
[9] Cusack N E 1978 *Metal–Nonmetal Transition in Disordered Systems* ed L R Friedman and D P Tunstall (Edinburgh: Scottish Universities Summer School of Physics) p 455
[10] Freyland W 1981 *Commun. Solid State Phys.* **10** 1
[11] Alekseev V A and Jakubov I T 1983 *Phys. Rep.* **96** 1
[12] Freyland W and Hensel F 1985 *The Metallic and the Nonmetallic States of Matter* ed P P Edwards and C N Rao (London: Taylor and Francis) p 93
[13] Endo H 1982 *Prof. Theor. Phys. Suppl.* **72** 100
[14] Hensel F 1987 *Large Finite Systems* ed J Jortner, A Pullmann and B Pullmann (Dordrecht: Reidel) p 345
[15] Gläser W, Hensel F and Lüscher E (ed) 1986 *Proc. 6th Int. Conf. on Liquid and Amorphous Metals* (München: Oldenbourg)
[16] Evans R 1970 *J. Phys. C: Met. Phys. Suppl.* **2** 137
[17] Hefner W, Schmutzler R W and Hensel F 1980 *J. Physique Coll.* **41** C8 62
[18] Even U and Jortner J 1972 *Phys. Rev. Lett.* **28** 31
[19] Warren W W and Hensel F 1982 *Phys. Rev.* B **26** 5980
[20] Mott N F 1966 *Phil. Mag.* **13** 989
[21] Ikezi H, Schwarzenegger K, Simons A L, Passner A L and McCall S L 1978 *Phys. Rev.* B **18** 2494
[22] Hefner W and Hensel F 1982 *Phys. Rev. Lett.* **48** 1026
[23] Overhof H, Uchtmann H and Hensel F 1976 *J. Phys. F: Met. Phys.* **6** 523
[24] Uchtmann H, Brusius U, Yao M and Hensel F 1988 *Z. Phys. Chem. NF* **156** 151
[25] Bhatt R N and Rice T M 1979 *Phys. Rev.* B **20** 466
[26] Uchtmann H, Popielawski J and Hensel F 1981 *Ber. Bunsenges. Phys. Chem.* **85** 555
[27] Pestak M W and Chang M H W 1981 *Phys. Rev. Lett.* **46** 939
[28] Ganteför G, Bröker G, Holub-Kappe E and Ding A 1989 *J. Chem. Phys.* **91** 7972
[29] Rademann K, Kaiser B, Even U and Hensel F 1987 *Phys. Rev. Lett.* **59** 2319
[30] Rademann K 1989 *Ber. Bunsenges. Phys. Chem.* **93** 653

[31] Brechignac C, Broyer M, Cahuzac Ph, Delacretaz G, Labastie P, Wolf J P and Wöste L 1985 *Chem. Phys. Lett.* **120** 559; 1988 *Phys. Rev. Lett.* **60** 275
[32] Schlauf M 1989 *Doctoral Thesis* University of Marburg
[33] Haberland H, Kornmeier H, Langosch H, Oschwald M and Tanner G 1990 *J. Chem. Soc. Faraday Trans.* at press
[34] Martens J, Uchtmann H and Hensel F 1987 *J. Phys. Chem.* **91** 2489
[35] Mott N F 1974 *Metal–Insulator Transitions* (London: Taylor and Francis)
[36] Hensel F, Jüngst S, Noll F and Winter R 1985 *Localisation and Metal Insulator Transitions* ed D Adler and H Fritsche (New York: Plenum) p 109
[37] Hensel F, Jünst S, Knuth B, Uchtmann H and Yao M 1986 *Physica* B **139** 90
[38] Freyland W 1979 *Phys. Rev.* B **20** 5140
[39] El-Hanany W, Brennert G F and Warren W W 1983 *Phys. Rev. Lett.* **50** 540
[40] Knuth B and Hensel F 1990 *High Pressure Res.* **5** 552
[41] Winter R, Bodensteiner T, Gläser W and Hensel F 1987 *Ber. Bunsenges. Phys. Chem.* **91** 1327
[42] Castleman A W and Keesee R G 1988 *Science* **241** 36
[43] Hernandez J P 1986 *Phys. Rev.* A **34** 1316
[44] Jüngst S, Knuth B and Hensel F 1985 *Phys. Rev. Lett.* **55** 2160
[45] Götzlaff W 1989 *Doctoral Thesis* University of Marburg
[46] Cailletet L and Mathias E C 1986 *C. R. Acad. Sci., Paris* **102** 1202
[47] Goldstein R E, Parola A, Ashcroft N A, Pestak M W, Chen M H W, deBruyn J R and Balzarin D A 1987 *Phys. Rev. Lett.* **58** 41
[48] Rowlinson J S 1970 *Adv. Chem. Phys.* **41** 1
[49] Mermin N D 1971 *Phys. Rev. Lett.* **26** 957
[50] Nicoll J F 1981 *Phys. Rev.* A **24** 2203
[51] Goldstein R and Ashcroft N E 1985 *Phys. Rev. Lett.* **55** 2164